Study of Liquation-Induced Crack Formation in A-286 Superalloy during Hot Rolling

SHIH-MING KUO, MING-YEN LI and YEONG-TSUEN PAN

New Materials Research & Development Department
China Steel Corporation

Liquation-induced crack formation of an iron-based Alloy A-286 during hot rolling was investigated. Observations by metallography, fractography, electron probe micro-analysis (EPMA), energy dispersive X-ray spectrometer (EDX) and high resolution transmission electron microscopy (HRTEM) showed that the partial melting of A-286 austenitic grain boundaries resulted in the crack nucleation and propagation upon hot deformation at a temperature of 1200°C. The hot-cracking mechanism involving the dissolution of TiC particle and grain boundary liquation is proposed in this study. The continuous liquid films along the grain boundary resulted in the severe intergranular fracture of A-286 billet due to the dramatic drop in ductility during hot rolling.

Keywords: A-286, Liquation, Iron-based alloy, Hot rolling

1. INTRODUCTION

Superalloys are used in the high temperature components of land and aero based gas turbines. The increasing demand for more power efficient gas turbines is encouraging the development of superalloys with a higher working temperature and better stability in harsh operating environments. Alloy A-286 superalloy is one of the iron-based superalloys widely used in the aeronautic and car industries for elevated temperature services. This alloy, with a tensile strength in range of 900~1250 MPa and a yield strength in range of 600~850 MPa, is nominally a 25 wt% Ni and 15% Cr austenitic alloy containing Ti, Al and other minor alloying additives[1,2]. The microstructure and mechanical properties of A-286 alloy are highly sensitive to metallurgical reactions and thermal-mechanical processing. Heat affected zone (HAZ) cracking degradation of nickel- based alloys, stainless steels, ferritic steels and iron-based supperalloys at elevated temperature has been investigated by using weldability testing technology[3-8]. Most of investigations into the effect of the HAZ welding process on metal alloys were, however, focused on the thermal effect of welding process[9-16]. Few comments have been made relating to liquation-induced crack formation during hot working. The occurrence of hot cracking in Alloy A-286 caused ruptures upon commercial mill rolling. To understand the mechanism responsible for A-286 hot cracking, a further study involving the influence of grain boundary liquation on the microstructural variation and fracture mechanism during hot rolling was carried out. In this study we also report on the liquation behavior of the grain boundary in an A-286 alloy under hot deformation at the temperature of 1200°C.

2. EXPERIMENTAL METHOD

An A-286 billet (Fe-25Ni-14Cr-2Ti-1.2Mo-1.1Mn-0.66Si-0.2V-0.03C-0.2Al) with dimensions of 220×260×8000 mm^3 was produced through the melting (Vacuum Induction Melting and Electro Slag Remelting) and forging processes. To achieve the uniform temperature distribution, the A-286 billet was heated up to 1200°C and held for 2 hours before hot rolling. The billet was rolled at the temperature of 1200°C with the reduction of 20% under the strain rate of 16.3 m/s. The temperature variation for the different positions of A-286 billet under hot rolling was calculated by using Deform *3-D* with the A-286's parameter of Young's modulus, Poisson's ratio, thermal conductivity and emissivity. Besides, the temperature of the A-286 billet was also monitored by an Infrared thermometer upon hot rolling.

The microstructure of each specimen was characterized with SEM (Scanning Electron Microscopy； JEOL JSM-7000F), EDX, EPMA (JEOL JXA-8900R) and HR-TEM (FEI E.O. Tecnai F20 G2 MAT S-TWIN). All specimens prior to SEM and EPMA examinations were mechanically polished with wet SiC abrasive paper down to 1 μm roughness and chemically etched

at room temperature in a 30 cc HCl, 30 cc HNO_3 and 20 cc H_2O solution for 1 minute. Thin foils specimens for TEM observation were prepared by the twin-jet electro-chemical polishing method in an electrolyte of 10% perchloric acid and 90% acetic acid. The fracture surface was examined by SEM.

3. RESULTS AND DISCUSSION

The microstructure of A-286 billet prior to hot rolling is shown in Fig.1. The precipitated phase shown in the austenite matrix is titanium carbonitrides, Ti(C,N), as identified with EDX and shown in Fig.1. After the rolling pass with the reduction of 20%, the material with about the one-sixth thickness of the billet in the upper surface was peeled and swirled due to severe cracking, as shown in Fig.2(a). After hot rolling, the observed intergranular fracture showed that the entire crack surface was covered by a thin layer of liquid, as shown in Fig.2(b). Fig.2(c) illustrates the cross-sectional SEM image of the rolled A-286 billet. After hot rolling at 1200°C, the nucleation and propagation of crack was found along the grain boundaries, which was induced by the intergranular partial melting involving the dissolution of TiC and localized melting at the grain boundary, as depicted in Fig.2(c). In this study, we propose two primary causes of the liquation that occurred at the grain boundaries involving constitutional liquation of TiC or Ti(C,N) and grain boundary liquation due to segregation of minor alloying elements during hot rolling. The mechanism of crack formation was also discussed in the following sections in this article.

3.1 Rolling-induced constitutional liquation of second phase particles

Constitutional liquation of carbides and sulfides has been proposed as the mechanism of HAZ cracking in several alloys such as Inconel 718, Hastelloy X, Incoloy 903, Incoloy 800 and Type 321 stainless steel [9-12]. It was reported that the constitutional liquation mechanism requires the reaction between a "constituent" particle and the surrounding matrix such that local melting occurs at the constituent particle/matrix interface, hence the term "constituent" liquation was used. Under the conditions of constitutional liquation, the constituent particle itself does not melt. Most of the particles that undergo constitutional liquation (such as NbC and TiC) have melting temperatures far exceeding that of the base metal. Rather, it is the intermediate composition in the reaction zone between the particle and the matrix that melts[3,7,12,15,16]. The particle reacts with the matrix to create a composition gradient around the particle, and the reaction zone composition undergoes melting below the melting temperature of the surrounding matrix. Therefore, the intergranular NbC

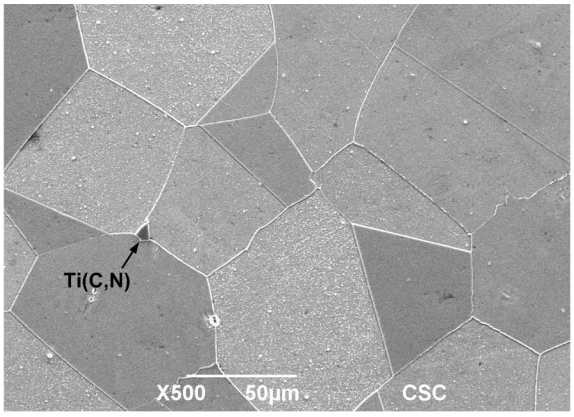

Fig.1. Microstructure of A-286 alloy before hot rolling.

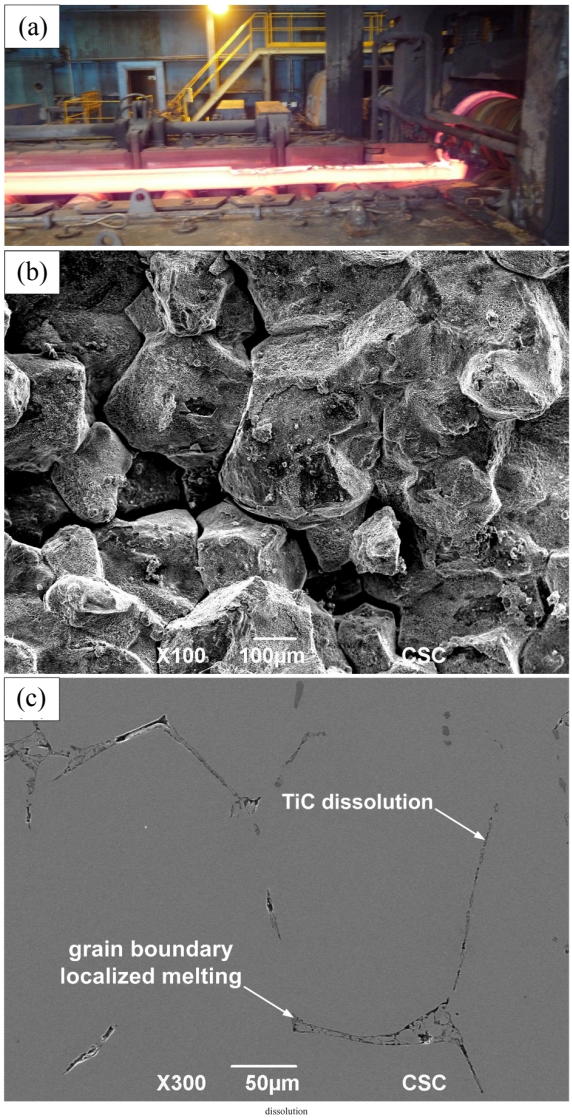

Fig.2. (a) Severe cracking of A-286 billet after mill-rolling at the temperature of 1200°C; (b) Fracture surface; and (c) Cross-sectional microstructure of A-286 billet after hot rolling.

or TiC was decomposed to release Nb or Ti to the matrix causing eutectic melting, and localized melting liquids spread along the grain boundaries.

EPMA line-scan analysis shows the element distribution profile at the liquidized grain boundary/matrix interface, as shown in Fig.3. The Ti and C enrichments at the grain boundary were due to the dissolution of TiC particles under hot-rolling, as shown in Fig.3(b). It was reported that the grain boundary melting results from a constitutional liquation driven by the eutectic reaction between the grain boundary TiC or Ti(C,N) and the matrix, namely, the Fe-Ti and/or Ni-Ti, eutectic reactions in austenitic stainless steel welds[7,15,16]. It was also reported that the melt phase nucleates largely around decomposing Mo-enriched TiC or Ti(C, N) in the HAZ of A-286 alloy[7,17,18]. In this study, however, Mo and N were not detected around the decomposition product of TiC after hot rolling, as shown in Fig.3(b).

3.2 Rolling-induced intergranular liquation due to segregation of melting point suppressant elements

Liquation of grain boundary materials can also be propelled by the segregation of melting point suppressant elements, which reduce the melting temperature of the grain boundary regions relative to the surrounding matrix. In general, grain growth can be induced by thermal energy through atomic diffusion under heat treatment, resulting in grain boundary migration. A moving boundary may sweep up the minor elements and impurities through a grain boundary sweeper mechanism[7,15,16]. Therefore, the concentration of solute elements and impurities at the grain boundary was enhanced after soaking at 1200°C for 2 hours.

On the other hand, the phenomenon of the solute and/or impurity elements segregating to the grain boundaries is driven by the free energy difference between a solute or impurity atom in a matrix site versus a grain boundary site. Since the defect density in a grain boundary is higher than that in the adjacent matrix, a tendency toward the grain boundary stabilization can be achieved by the diffusion of atoms to the boundary sites. Segregation (compositional inhomogeneity) was induced through the migration of solute or impurity elements to the grain boundary by the heating process. Therefore, a lower temperature allowing the occurrence of liquation could be expected at the grain boundary rather than in the surrounding matrix. It was reported that the liquation cracking in the HAZ of Inconel 718 alloy was induced due to the segregation of boron and phosphorus, which significantly decreased the resistance to cracking[12,16,19-21]. In this study, the segregation of S was detected at the grain boundaries, as shown in Fig.3(b), which would rapidly lower the local melting temperature, and more extensive liquation and cracking were found when TiC and S coexisted at the grain boundary, suggesting a synergetic effect during hot rolling.

Generally, grain boundaries contain higher levels of impurities and minor elements and exhibit a higher defect density. From a free energy viewpoint, liquation will always occur first at the grain boundaries. The effective melting temperature of an alloy varies because of the localized variations in the solute or minor element contents. Both impurity elements, such as sulfur and phosphorus, and minor alloy elements, such as boron, silicon, titanium and niobium, promote hot cracking in austenitic steels[12,15-18]. It was reported that the HAZ microfissuring was induced by the eutectic reaction between laves phase (Fe_2Mo, Fe_2Ti, $(Fe,Ni)_2Ti$ or $(Mo,Ti)(Fe,Cr,Si)_2$) and the austenitic matrix due to the low eutectic melting temperature (Eutectic Fe-Fe_2Ti：1290°C；Eutectic Fe-Fe_2Si：1212°C) in Alloy A-286[7,17,18]. Grain boundary wetting would be enhanced under an applied stress, where induced capillary action

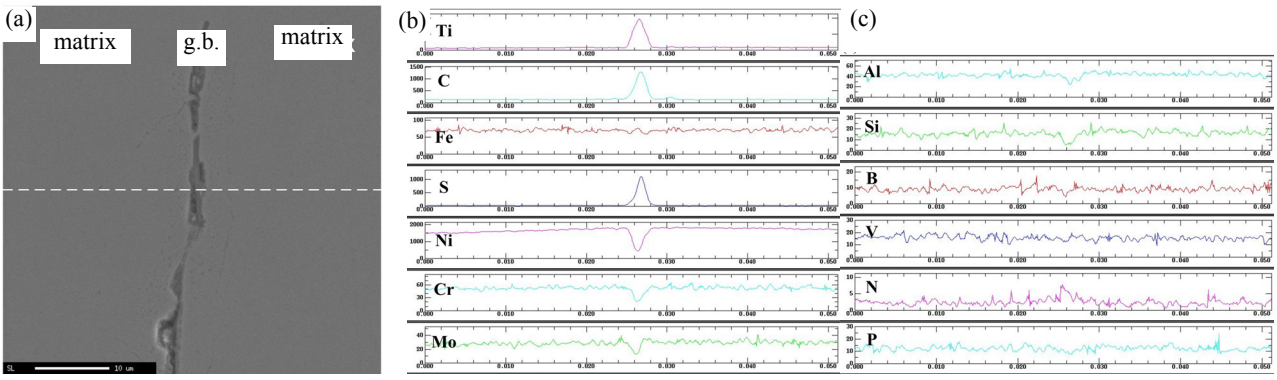

Fig.3. EPMA line-scan analysis for the dissolution of TiC at the grain boundary of A-286 billet after hot rolling. (a) SEM cross-sectional picture at the liquation grain boundary/matrix interface; (b) EPMA line-scan analysis of Ti, C, Fe, S, Ni, Cr and Mo elements distribution profile in Fig.3(a); and (c) EPMA line-scan analysis of Al, Si, B, V, N and P elements distribution profile in Fig.3(a).

would spread the liquid along grain boundaries[22,23]. Therefore, it might be a possible reason for causing the localized melting liquation at the grain boundary between the matrix grains after hot rolling, shown in Fig.4(a), although the Laves phase was not observed in this study.

TEM-EDX analysis shows the composition of the intergranular liquid layer after hot rolling, which contains 21.3% (atomic percent) of Cr, 2.6% of Si, 1.5% of Al, 4.9% of C, 0.6% of Ti, 0.9% of Mo and 24.9% of Ni, as shown in Fig.4(b). The segregation of Si and Ti may lower the melting temperature of the grain boundary since both elements form low melting eutectics with Fe and Ni. Therefore, it was reported that the fusion cracking zone was highly enriched with Ni, Ti, Si and Mo in Alloy A-286 after heating at 1350°C for 2 hours[7,18]. Besides, the segregation of B, S and P might cause a local depression of the melting temperature and promote the formation of continuous liquid films along these boundaries, although they were not directly detected according to the TEM observations. Therefore, the local melting of grain boundaries might occur at a temperature below the melting point of the surrounding matrix during hot rolling, as shown in Fig.4(a).

The mechanism of intragranular liquation due to the segregation of melting point suppressing elements may dominate the liquation process due to a small amount of Ti(C,N) and/or TiC precipitation at the grain boundary for the A-286 alloy. Therefore, the hot ductility behavior and hot cracking were significantly improved by reducing Si, B and Mn additions in Alloy A-286[17]. It has been reported that intergranular cracking was induced by the liquid-metal embrittlement based on the capillary-transport mechanism in Type 304 stainless steel[22]. For the irregular intergranular path encountered with the cracking, the liquid-metal atoms penetrating at the capillary-transport velocity, V, can be related to crack length, L, by the following expression (when the appropriate correction factor for the intergranular path of the crack is applied) :

$$V=\frac{Tr\cos\theta}{3\pi\mu L}$$

Where T is the surface tension of the liquid, r is the distance between the crack surfaces, θ is the contact angle, and μ is the coefficient of viscosity. The capillary-transport of liquid-metal atoms would be enhanced by the shear stress with high strain rate under the application of external stress[22,23]. Therefore, rolling-induced shear stress would cause continuous boundaries covered with the liquid layers resulting in the severe intergranular fracture of Alloy A-286 billet as a result of the dramatic drop in ductility during hot rolling, as shown in Fig.2(b).

It is observed that numerous nano-size particles (with the dimensions of 20~30 nm) precipitated at the liquidized grain boundary/matrix interface after hot rolling, as shown in Fig.4(a). Fig.4(c) shows the HRTEM image of the liquation interface (area A of Fig.4(a)) between the localized melting grain boundary and the matrix after hot rolling. The TEM analysis shows that the precipitated grains (grain 2 and 3) adjacent to the grain boundary possess the same FCC (face-center-cubic) structure as the matrix (γ phase) with the close-packed plane of (111). After hot deformation, grain 2 (distance of plan (111) d_{111} = 2.08°A) was formed at the interface between grain 1(distance of plan (111) d_{111} = 2.10°A) and the grain boundary, as shown in Fig.4(c). It exhibits an angle of around 40° between grain 1 and 2, since grain 2 might crystallize along the direction of thermal conduction during cooling. As there was not enough time for the long-range order process of crystallization owing to the fast cooling procedure, the amorphous structure of the residual melting phase was solidified with the thickness of 5 nm at the interface between grain 2 and 3 after hot rolling, as shown in Fig.4(c).

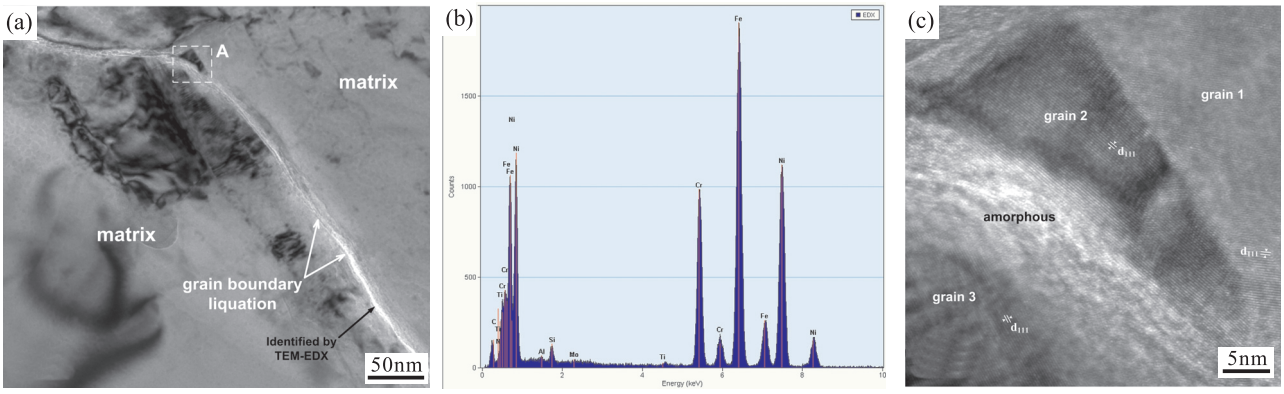

Fig.4. (a)TEM image for the local-melting at the grain boundary of A-286 billet after hot rolling; (b)TEM-EDX analysis for the intergranular liquid layer in Fig.4(a); and (c) HRTEM image of the liquation interface (area A of Fig.4(a)) between the liquidized grain boundary and the matrix.

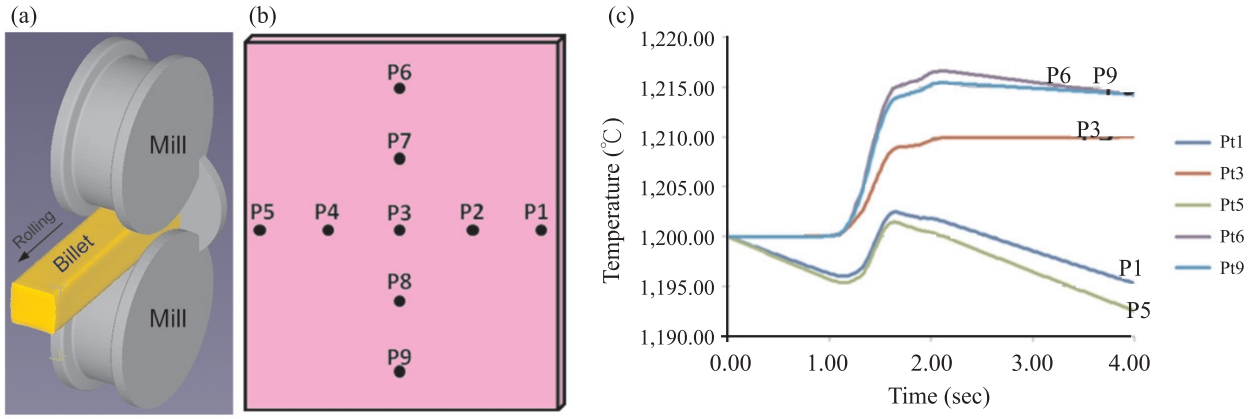

Fig.5. (a) Schematic diagram of A-286 billet (220(H)×260(W)×8000(L) mm^3) during hot rolling; (b) Schematic cross-section positions of A-286 billet; and (c) Temperature variation for the different positions of A-286 billet in Fig.5(b) upon hot rolling according to the simulated calculation.

3.3 Rolling-induced local heating giving rise to crack nucleation

The mechanical history with a relatively large amount of external stress during hot rolling is a different scenario from the welding situation. Simulated calculation data shows that the local temperature increases in the Alloy A-286 billet are due to the additional heat produced by the transformation of mechanical energy to heat energy during hot rolling, as shown in Fig.5. Besides, the temperature increase of 15~30°C for the A-286 billet was measured by an Infrared thermometer during hot rolling. The temperatures at positions 6 and 9 are higher than those at positions 1 and 5, while the temperatures at positions 2, 4, 7 and 8 lie between the positions 9 (position 6) and 3, as shown in Fig.5(c). A temperature increase of more than 15°C was generated in positions 6 and 9 of the billet when rolling deformation was occurring. Stress-induced local heating would aggravate the grain boundary liquation behavior, as described in 3.1 and 3.2. Therefore, cracks nucleated from the one-sixth thickness of the A-286 billet in the upper surface of the billet (positions 6 or 9) and propagated along the liquidized locations under loading rolling stress, as shown in Fig.2(a).

4. CONCLUSIONS

1. Rolling-induced partial melting within the austenitic grain boundaries of an iron-based A-286 superalloy results from the TiC dissolution and intragranular localized melting after mill-rolling at a temperature of 1200°C. The continuous liquid films formed along the grain boundary gives rise to the dramatic drop in ductility, resulting in the rapid crack propagation during hot rolling.
2. EPMA analysis shows that the Ti and C enrichments at the grain boundary were due to the decomposition of TiC, and more extensive liquation and cracking were driven by the synergetic effect of the constitutional liquation of TiC and the segregation of S at the grain boundary during hot rolling.
3. TEM analysis shows that many nano-size crystallized γ grains with the close-packed plane of (111) were precipitated at the interface between the amorphous grain boundary and the austenitic matrix after hot rolling.
4. Rolling-induced local heating (>15°C) at a one-sixth depth of the A-286 billet in the upper surface resulted in the crack nucleation and propagation along the liquidized grain boundary upon hot deformation at the temperature of 1200°C.

REFERENCES

1. A. W. Tompson and J. A. Brooks: Metall. Trans. A, 1975, vol. 6, pp. 1431-1442.
2. J. A. Brooks and A. W. Tompson: Metall. Trans. A, 1993, vol. 24, pp. 1983-1991.
3. R. G. Thompson and S. Genculu: Welding Research Supplement, 1983, vol. 62, pp. 337s-345s.
4. F. F. Noecker and J. N. Dupont: Welding Journal, 2009, vol. 88, pp. 7-20.
5. W. F. Savage, E. F. Nippes and G. M. Goodwin: Welding Research Supplement, 1977, vol. 56, pp. 245-253.
6. J. C. Lippold: Welding Research Supplement, 1984, vol. 63, pp. 91-103.
7. A. D. Romig, J. C. Lippold and M. J. Cieslak: Metall. Trans. A, 1988, vol. 19, pp. 35-50.
8. H. Guo, M. C. Chaturvedi, N. L. Richards and G. S. Mcmahon : Scripta Materialia, 1999, vol. 40, pp. 383-388.

9. J. C. Lippold, W. A. Baeslack and I. Varol : Welding Research Supplement, 1992, vol. 50, pp. 1s-11s.
10. M. Qian and J. C. Lippold : Acta Materialia, 2003, vol. 51, pp. 3351-3361.
11. R. Nakkalil, N. L. Richards and M. C. Chaturvedi : Acta Materialia, 1993, vol. 41, pp. 3381-3392.
12. S. L. West, W. A. Baeslack and T. J. Kelly: Metalloygraphy, 1989, vol. 23, pp. 219-229.
13. S. M. Mousavizade, F. M. Ghaini, M. J. Torkamany, J. Sabbaghzadeh and A. Abdollahzadeh: Scripta Materialia, 2009, vol. 60, pp. 244-247.
14. R. I. Hsieh, S. C. Wang and H. Y. Liou : China Steel Technical Report, 1993, vol. 7, pp. 38-44.
15. B. Radhakrishnan and R. G. Thompson : Metalloygraphy, 1988, vol. 21, pp. 453-471.
16. V. Shankar, T. P. Gill, S. L. Mannan and S. Sundaresan: Sadhana, 2003, vol. 28, pp. 359-382.
17. J. A. Brooks: Welding Research Supplement, 1974, vol. 53, pp. 517s-523s.
18. J. A. Brooks and R. W. Krenzer: Welding Journal, 1974, vol. 53, pp. 242s-245s.
19. J. J. Pepe and W. F. Savage : Welding Research Supplement, 1970, vol. 49, pp. 545s-553s.
20. W. F. Savage and B. M. Krantz : Welding Research Supplement, 1971, vol. 50, pp. 292s-303s.
21. W. F. Savage, E. F. Nippes and T. W. Miller: Welding Research Supplement, 1976, vol. 55, pp. 181s-187s.
22. W. F. Savage, E. F. Nippes, and M. C. Mushala: Welding Research Supplement, 1978, vol. 57, pp. 237s-245s.
23. S. J. Matthews and W. F. Savage: Welding Research Supplement, 1971, vol. 50, pp. 174s-182s. □